J Mater Sci (2008) 43:5385–5389
DOI 10.1007/s10853-008-2806-8

Modifying the oxygen adsorption properties of $YBaCo_4O_7$ by Ca, Al, and Fe doping

Song Wang · Haoshan Hao · Baofeng Zhu · Jianfeng Jia · Xing Hu

Received: 23 March 2008 / Accepted: 13 June 2008 / Published online: 28 June 2008

Abstract The doping effect of Ca, Al, and Fe on the oxygen adsorption properties of $YBaCo_4O_7$ was investigated by thermogravimetry (TG) method. It was found that the original $YBaCo_4O_7$ oxygen adsorption properties can be modified greatly by Ca, Al, and Fe doping. Ca doping in Y sites eliminates the oxygen adsorption at low temperature ($\sim$300 °C) but the oxygen adsorption properties at high temperature is almost unchanged. Minor Al doping in Co sites eliminates the oxygen adsorption hump at high temperature, but the hump at low temperature is preserved. Fe appearance in $YBaCo_3Al_{1-x}Fe_xO_7$ seems to weaken the effect of Al doping, so the oxygen hump at high temperature emerges again. The doping effect was discussed based on elements valence, binding energy between cations and oxygen ions, and distortion of crystal structure.

Introduction

Oxygen content in many transition metal oxides is tunable with the temperature and surrounding oxygen partial pressure because of the variable valence state of transition metals. This oxygen nonstoichiometry makes it possible for oxygen ions to be adsorbed/desorbed on the surface or diffuse in the bulk materials, which has been utilized in fields such as solid-oxide fuel cells, gas-separation membranes, and oxygen sensors. Recently, a new class of transition metal oxides $RBaCo_4O_7$ (R represents rare earth elements) have been synthesized by Valldor and Andersson [1, 2]. Since then, studies on their structure, magnetic and electronic properties have been carried on by several groups [3–10]. The crystal structure of $RBaCo_4O_7$ is built up of Kagomé sheets of CoO_4 tetrahedra, linked by triangular layers of CoO_4 tetrahedra [3–5]. The ratio of Co ion numbers in the kagomé- and triangular-lattices is 3 to 1 and the valences of Co ions are mixed consisting of three Co^{2+} ions and one Co^{3+} ion. It has been reported that $RBaCo_4O_7$ oxides experience two oxygen adsorption and subsequent desorption processes when heated from room temperature to 1100 °C in air or oxygen, the first being around 200–450 °C, and the other around 650–1050 °C [11, 12]. The weight change caused by the oxygen gain is up to about 4% of its original weight. The adsorbed oxygen atoms at low temperature primarily bond with some of the cobalt ions and the Co octahedra form by the addition of extra oxygen atoms in $YBaCo_4O_{8.1}$ [13]. However, oxygen adsorption at high temperature completely destroys the crystal structure of $RBaCo_4O_7$ and decomposes $RBaCo_4O_7$ to other phases [11, 12, 14]. In this work, we synthesized Ca, Al, and Fe-doped $(Y,Ca)Ba(Co,Al,Fe)_4O_7$ compounds and investigated the effect of element doping on the oxygen adsorption properties of $YBaCo_4O_7$.

Experimental

The compositions $Y_{1-x}Ca_xBaCo_4O_7$ ($0 \le x \le 1$), $YBaCo_{4-x}Al_xO_7$ ($0 \le x \le 1$), and $YBaCo_3Al_{1-x}Fe_xO_7$ ($0.2 \le x \le 1$) were prepared by the solid-state reaction method. The stoichiometric mixture of Y_2O_3, $CaCO_3$, $BaCO_3$, Co_3O_4, Al_2O_3, and Fe_2O_3 was slowly heated up to 1000 °C and held

S. Wang · H. Hao · B. Zhu · J. Jia · X. Hu (✉)
School of Physical Engineering and Material Physics Laboratory, Zhengzhou University, Zhengzhou 450052, China
e-mail: xhu@zzu.edu.cn

H. Hao
Department of Mathematical and Physical Sciences, Henan Institute of Engineering, Zhengzhou 451191, China

for 10 h at this temperature in a box furnace. The calcined powder was reground, pressed into pellets, and sintered at 1050–1160 °C in air for 20 h once again. Then the sintered samples were quenched to room temperature to avoid the oxygen adsorption in the cooling stage.

X-ray diffraction (XRD) analysis was carried out with X'tert Pro system using Cu Kα radiation. Oxygen content of the as-synthesized samples was determined by iodometric titration and the results show that the value is very close to 7 for all compositions. Thermogravimetry (TG) measurements were performed with a thermo-analyzer (SETARAM, Labsys^{TM}) to investigate the oxygen adsorption properties of the samples. In these experiments about 60 mg powder sample was put in an alumina crucible and heated from room temperature to 1100 °C with a heating rate 5 °C/min in 30 mL/min oxygen flow.

Results

Ca doping in $Y_{1-x}Ca_xBaCo_4O_7$

Figure 1 shows the XRD patterns of $Y_{1-x}Ca_xBaCo_4O_7$ ($0 \leq x \leq 1$) powder samples. The main phase is the dominating phase or the only phase in the powder indexed as $YBaCo_4O_7$ structure [1, 2]. Only in $CaBaCo_4O_7$ do some little impurities present, which seems as a mix of CaO_2, CoO, and $Ca_3Co_4O_9$ (indicated as * in Fig. 1) and cannot be identified as one single impurity phase.

Figure 2 shows the weight change of $Y_{1-x}Ca_xBaCo_4O_7$ when heated in oxygen from room temperature to 1100 °C. As seen in Fig. 2, TG curve of $YBaCo_4O_7$ exhibits two prominent humps due to oxygen gain and subsequent oxygen loss, being consistent with previous reports

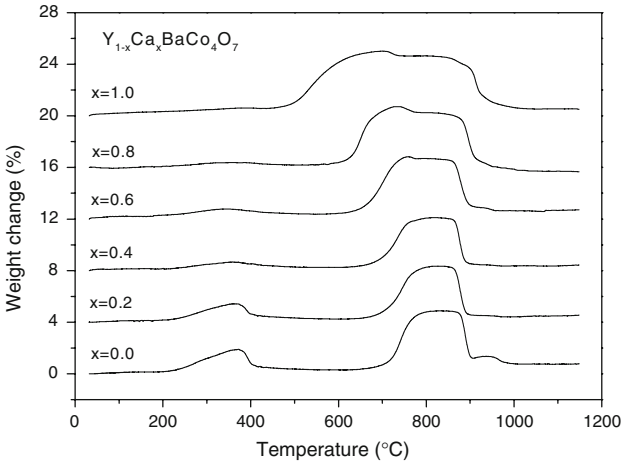

Fig. 2 Weight change of $Y_{1-x}Ca_xBaCo_4O_7$ with temperature in oxygen

[11, 12]. Compared with $YBaCo_4O_7$, Ca doping in $Y_{1-x}Ca_xBaCo_4O_7$ leads to two significant changes on the oxygen adsorption behavior. On the one hand, the amount of adsorbed oxygen at low temperature is reduced with the increase of Ca concentration. Especially for $CaBaCo_4O_7$, its low-temperature oxygen adsorption hump almost disappears. On the other hand, the amount of adsorbed oxygen at high temperature is almost unchanged for all compositions (about 4% of its original weight), but the beginning temperature of oxygen adsorption decreases with the increase of Ca concentration, from 650 °C for $YBaCo_4O_7$ to 440 °C for $CaBaCo_4O_7$.

Al doping in $YBaCo_{4-x}Al_xO_7$

XRD patterns of $YBaCo_{4-x}Al_xO_7$ ($0 \leq x \leq 1$) in Fig. 3 show that Co can be substituted by minor Al and no second

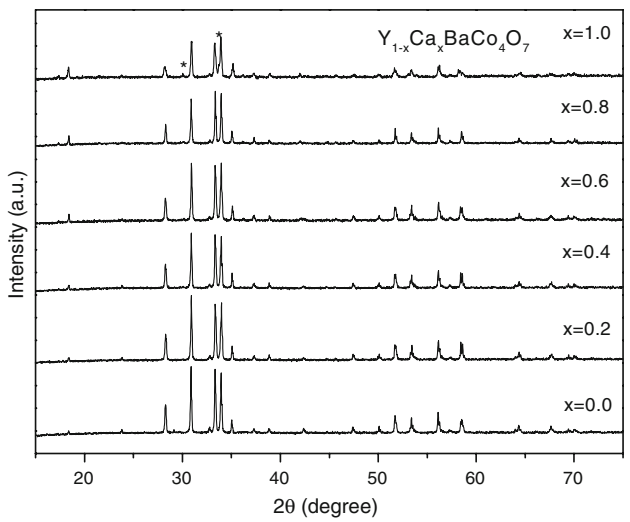

Fig. 1 XRD patterns of $Y_{1-x}Ca_xBaCo_4O_7$

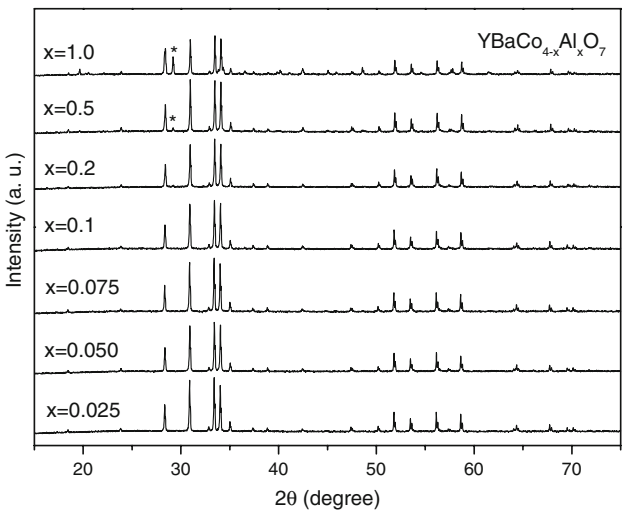

Fig. 3 XRD patterns of $YBaCo_{4-x}Al_xO_7$

Table 1 Cell parameters and cell volumes of $YBaCo_{4-x}Al_xO_7$ and $YBaCo_3Al_{1-x}Fe_xO_7$

Sample	a (Å)	c (Å)	V (Å^3)
$YBaCo_4O_7$	6.299	10.235	351.68
$YBaCo_{3.9}Al_{0.1}O_7$	6.294	10.231	351.05
$YBaCo_{3.8}Al_{0.2}O_7$	6.289	10.229	350.15
$YBaCo_3Al_{0.5}Fe_{0.5}O_7$	6.294	10.247	351.55
$YBaCo_3FeO_7$	6.306	10.257	353.27

phase was detected for the samples with $x \leq 0.2$. Impurity phases appear with the further increase of Al concentration and it can be identified as Y_2O_3 (indicated as * in Fig. 3).The calculated cell dimension presented in Table 1 shows that Al doping decreases cell parameters and cell volumes due to smaller ionic radii of Al^{3+} with respect to Co^{3+} [15].

TG curves of $YBaCo_{4-x}Al_xO_7$ heated in oxygen were presented in Fig. 4. One can see that, for $x \leq 0.1$ samples, their oxygen adsorption behavior at low temperature is not influenced by Al doping, but the amount of adsorbed oxygen at high temperature is rapidly reduced with the increasing Al concentration. When $x \geq 0.2$, the high-temperature hump disappears and the height of the hump at low temperature is also lowered. Moreover, the beginning temperature of the high-temperature hump increases with the increasing Al concentration, from 650 °C for Al-free sample to 780 °C for $x = 0.1$ sample.

Al and Fe co-doping in $YBaCo_3Al_{1-x}Fe_xO_7$

Figure 5 shows the XRD patterns of $YBaCo_3Al_{1-x}Fe_xO_7$ ($0.2 \leq x \leq 1$) powder samples. The substitution solubility of Fe for Co can reach $x = 1.0$, corresponding to one fourth Co lattice sites. Moreover, the presence of Fe seems to increases the solubility of Al in the Co site, so the samples with $x \geq 0.5$ (corresponding to Al concentration $\leq$12.5%) are the pure phase and impurities begin to appear for the $x = 0.2$ sample, which is also Y_2O_3 (indicated as * in Fig. 5). As seen in Table 1, Fe doping leads to the increase of cell dimension due to larger ionic radii of Fe^{3+} with respect to Co^{3+} and Al^{3+} [15].

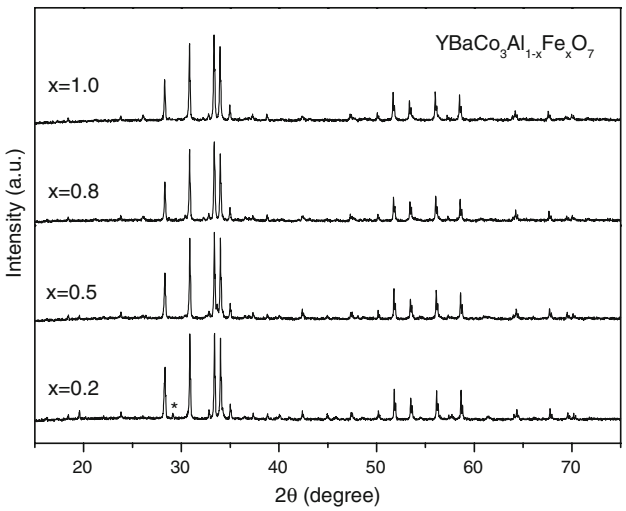

Fig. 5 XRD patterns of $YBaCo_3Al_{1-x}Fe_xO_7$

Figure 6 shows the relationship of weight change with temperature for $YBaCo_3Al_{1-x}Fe_xO_7$ in oxygen. The presence of Fe in the Co site seems to weaken the effect of Al doping, so the oxygen adsorption at high temperature emerges again, and the height of the hump increases with the increasing Fe concentration. Moreover, the beginning temperature of oxygen adsorption at high temperature decreases with the increase of Fe concentration, from 820 °C for $x = 0.2$ sample to 720 °C for $x = 1.0$ sample.

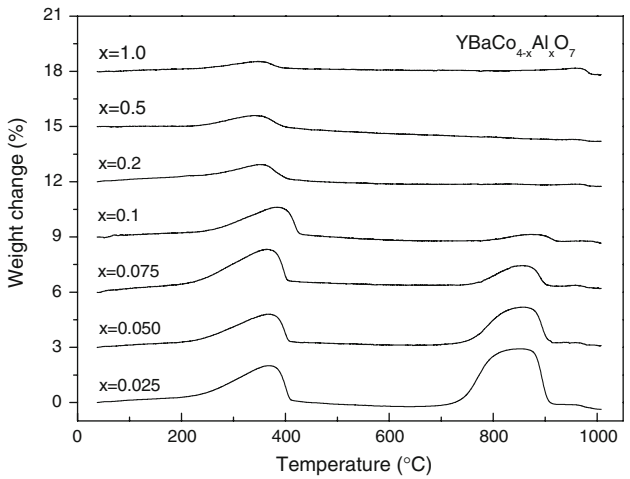

Fig. 4 Weight change of $YBaCo_{4-x}Al_xO_7$ with temperature in oxygen

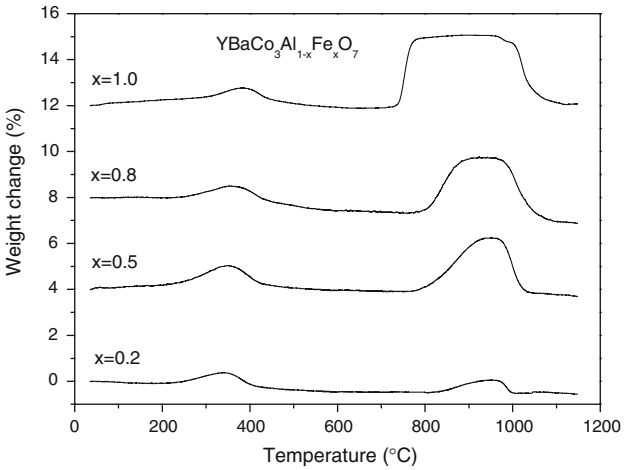

Fig. 6 Weight change of $YBaCo_3Al_{1-x}Fe_xO_7$ with temperature in oxygen

Compared with undoped $YBaCo_4O_7$, however, Fe doping increases the beginning temperature of oxygen adsorption of $YBaCo_3FeO_7$.

Discussion

In $YBaCo_4O_7$, all four Co ions are located in CoO_4 tetrahedra and the Co^{2+}/Co^{3+} ratio is 3 to 1. Chmaissem et al. [13] have verified that the Co octahedra form by the addition of extra oxygen atoms in $YBaCo_4O_{8.1}$. The extra oxygen atoms enter the structure to bond with half of the triangular cobalt ions and form zigzag patterns of Co(1)-octahedra. In the Kagomé layer, Co(2)-octahedra form directly above and below the Co(1)-octahedra to form zigzag ribbons directed along the c-axis. Therefore, Co ions occupy both corner-sharing tetrahedral and edge-sharing octahedral sites in $YBaCo_4O_{8.1}$. All octahedral Co ions and their surrounding first neighbor tetrahedral Co ions are trivalent. Bivalent corner-sharing Co tetrahedral form continuous zigzag ribbons in the b-axis direction, linking the chains of Co^{3+} polyhedra.

In the case of Ca-doped $Y_{1-x}Ca_xBaCo_4O_7$, there still have seven oxygen per every formula unit for the air-synthesized compounds [2, 16, 17] and our titration experiment also confirm this result. This means that the introduction of Ca^{2+} cation on Y^{3+} site will be electronically compensated by the oxidation of Co ions from the divalent state to the trivalent state. The decrease of the amount of Co^{2+} ions may be responsible for the decrease of adsorbed oxygen in $Y_{1-x}Ca_xBaCo_4O_7$ in the lower temperature range.

When Co^{3+} ions is substituted by minor Al^{3+} ($\leq$2.5%) in $YBaCo_{4-x}Al_xO_7$, one can expect that the amount of Co^{2+} ions and thus the oxygen adsorption capacity would not be influenced by this isovalent substitution. As a result, the low-temperature oxygen adsorption of Al-doped $YBaCo_{4-x}Al_xO_7$ ($x \leq 0.1$) is similar to that of undoped $YBaCo_4O_7$. The drop of the amount of adsorbed oxygen for $x \geq 0.2$ samples may be related to the presence of impurities. Similarly, Fe^{3+} substituting for Co^{3+} or/and Al^{3+} in $YBaCo_3Al_{1-x}Fe_xO_7$ would not influence the amount of Co^{2+} ions (here assuming Fe ions being trivalent in these compounds [2]), so Fe doping has little effect on the oxygen adsorption behavior.

Pervious studies have verified that $YBaCo_4O_7$ phase is thermodynamically instable under oxidizing condition in the temperature range 650–950 °C and oxygen adsorption in this temperature range will decompose $YBaCo_4O_7$ into several other phases [11, 12, 14]. Therefore, the change of the beginning temperature of oxygen adsorption at high temperature means the change of decomposition temperature. As mentioned in the result section, Ca doping decreases the decomposition temperature of $Y_{1-x}Ca_xBaCo_4O_7$ and Al/Fe doping increases the decomposition temperature of $YBaCo_{4-x}Al_xO_7$ and $YBaCo_3Al_{1-x}Fe_xO_7$. Moreover, the disappearance of oxygen-adsorption hump for $YBaCo_{4-x}Al_xO_7$ with $x \geq 0.2$ indicates that these compositions are thermodynamically stable in oxygen atmosphere. However, the replacement of Al with Fe in $YBaCo_3Al_{1-x}Fe_xO_7$ tends to decreases the stability and the oxygen adsorption is preserved for the Fe and Al co-doped samples. To verify that Al doping can improve the phase stability, $YBaCo_4O_7$ and Al-doped samples were heat-treated at 850 °C in oxygen and then their XRD patterns were taken and presented in Fig. 7. One can see that oxygen adsorption at the high temperature destroys the $YBaCo_4O_7$ phase completely. The noticeable peak in the XRD pattern can be identified as (0 6 0) peak of $BaCoO_{3-x}$. However, with the increase of Al concentration, $YBaCo_4O_7$ phase appears again and becomes main phase in $x = 1.0$ sample, which indicates that Al doping can suppress the oxygen adsorption and phase decomposition at high temperature.

The effect of element doping on the lattice stability can be qualitatively understood on the basis of the change of bond energy between cations and oxygen ions. The bond energy of Ca–O is smaller than Y–O [18], so the lattice instability is enhanced by the replacement of Y cations by Ca cations. On the contrary, due to greater bond energy of Fe–O and Al–O than Co–O [19, 20], Al and Fe doping leads to the increase of lattice stability. By comparison, Al–O bond is relatively stronger compared to Fe–O [19], so Fe substituting for Al in $YBaCo_3Fe_{1-x}Al_xO_7$ decreases their lattice stability.

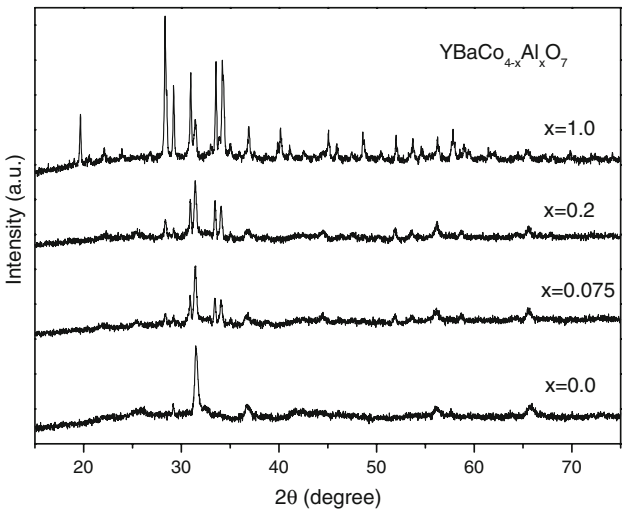

Fig. 7 XRD patterns of $YBaCo_{4-x}Al_xO_7$ after heat treatment at 800 °C in oxygen

Conclusion

Ca doping in $Y_{1-x}Ca_xBaCo_4O_7$ decreases the amount of adsorbed oxygen at the low temperature, whereas Al and/or Fe doping in $YBaCo_{4-x}Al_xO_7$ and $YBaCo_3Al_{1-x}Fe_xO_7$ has little effect on their low-temperature oxygen adsorption. The amount of adsorbed oxygen at the high temperature in $Y_{1-x}Ca_xBaCo_4O_7$ is not changed by Ca doping, but the decomposition temperature decreases with the increasing Ca concentration, indicating that the stability is reduced by Ca doping. Al doping in $YBaCo_{4-x}Al_xO_7$ decreases the amount of the adsorbed oxygen at high temperature and the stability increases with the increasing Al concentration. Fe appearance in $YBaCo_3Al_{1-x}Fe_xO_7$ weakens the effect of Al doping on the oxygen adsorption, so the oxygen adsorption at high temperature emerges again. Our results show that the two oxygen adsorption/desorption processes of $YBaCo_4O_7$ can be modulated separately by element doping, which is helpful for the understanding and the utilization of the unique oxygen adsorption properties of $RBaCo_4O_7$.

References

1. Valldor M, Andersson M (2002) Solid State Sci 4:923. doi:10.1016/S1293-2558(02)01342-0
2. Valldor M (2004) Solid State Sci 6:251. doi:10.1016/j.solidstatesciences.2004.01.004
3. Huq A, Mitchell JF, Zheng H, Chapon LC, Radaelli PG, Knight KS et al (2006) J Solid State Chem 179:1136. doi:10.1016/j.jssc.2006.01.010
4. Maignan A, Caignaert V, Pelloquin D, Hébert S, Pralong V, Hejtmanek J et al (2006) Phys Rev B 74:165110. doi:10.1103/PhysRevB.74.165110
5. Chapon LC, Radaelli PG, Zheng H, Mitchell JF (2006) Phys Rev B 74:172401. doi:10.1103/PhysRevB.74.172401
6. Hao H, Chen C, Pan L, Gao J, Hu X (2007) Phys B 387:98. doi:10.1016/j.physb.2006.03.089
7. Hao H, Zhang X, He Q, Chen C, Hu X (2007) Solid State Commun 141:591. doi:10.1016/j.ssc.2007.01.005
8. Tsipis EV, Khalyavin DD, Shiryaev SV, Redkina KS, Nunez P (2005) Mater Chem Phys 92:33. doi:10.1016/j.matchemphys.2004.12.027
9. Nakayama N, Mizota T, Ueda Y, Sokolov AN, Vasiliev AN (2006) J Magn Magn Mater 300:98. doi:10.1016/j.jmmm.2005.10.041
10. Caignaert V, Maignan A, Pralong V, Hebert S, Pelloquin D (2006) Solid State Sci 8:1160
11. Karppinen M, Yamauchi H, Otani S, Fujita T, Motohashi T, Huang Y-H et al (2006) Chem Mater 18:490. doi:10.1021/cm0523081
12. Hao H, Cui J, Chen C, Pan L, Hu J, Hu X (2006) Solid State Ionics 177:631. doi:10.1016/j.ssi.2006.01.030
13. Chmaissem O, Zheng H, Huq A, Stephens PW, Mitchell JF (2008) J Solid State Chem 181:664. doi:10.1016/j.jssc.2007.12.016
14. Tsipis EV, Kharton VV, Frade JR (2006) Solid State Ionics 177:1823. doi:10.1016/j.ssi.2006.03.037
15. Shannon RD (1976) Acta Crystallogr A 32:751. doi:10.1107/S0567739476001551
16. Valldor M (2006) Solid State Sci 8:1272. doi:10.1016/j.solidstatesciences.2006.05.014
17. Schweika W, Valldor M, Lemmens P (2007) Phys Rev Lett 98:067201. doi:10.1103/PhysRevLett.98.067201
18. Shao ZP, Xiong GX, Yang WS (2001) J Inorg Mater 16:23
19. Yaremchenko AA, Patrakeev MV, Kharton VV, Marques FMB, Leonidov IA, Kozhevnikov VL (2004) Solid State Sci 6:357. doi:10.1016/j.solidstatesciences.2004.01.005
20. Katsuki M, Wang S, Dokiya M, Hashimoto T (2003) Solid State Ionics 156:453. doi:10.1016/S0167-2738(02)00733-6